NASA/TM—2004–213175

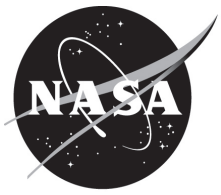

Analytical Modeling and Test Correlation of Variable Density Multilayer Insulation for Cryogenic Storage

L.J. Hastings
Alpha Technology, Inc., Huntsville, Alabama

A. Hedayat and T.M. Brown
Marshall Space Flight Center, Marshall Space Flight Center, Alabama

May 2004

The NASA STI Program Office…in Profile

Since its founding, NASA has been dedicated to the advancement of aeronautics and space science. The NASA Scientific and Technical Information (STI) Program Office plays a key part in helping NASA maintain this important role.

The NASA STI Program Office is operated by Langley Research Center, the lead center for NASA's scientific and technical information. The NASA STI Program Office provides access to the NASA STI Database, the largest collection of aeronautical and space science STI in the world. The Program Office is also NASA's institutional mechanism for disseminating the results of its research and development activities. These results are published by NASA in the NASA STI Report Series, which includes the following report types:

- TECHNICAL PUBLICATION. Reports of completed research or a major significant phase of research that present the results of NASA programs and include extensive data or theoretical analysis. Includes compilations of significant scientific and technical data and information deemed to be of continuing reference value. NASA's counterpart of peer-reviewed formal professional papers but has less stringent limitations on manuscript length and extent of graphic presentations.

- TECHNICAL MEMORANDUM. Scientific and technical findings that are preliminary or of specialized interest, e.g., quick release reports, working papers, and bibliographies that contain minimal annotation. Does not contain extensive analysis.

- CONTRACTOR REPORT. Scientific and technical findings by NASA-sponsored contractors and grantees.

- CONFERENCE PUBLICATION. Collected papers from scientific and technical conferences, symposia, seminars, or other meetings sponsored or cosponsored by NASA.

- SPECIAL PUBLICATION. Scientific, technical, or historical information from NASA programs, projects, and mission, often concerned with subjects having substantial public interest.

- TECHNICAL TRANSLATION. English-language translations of foreign scientific and technical material pertinent to NASA's mission.

Specialized services that complement the STI Program Office's diverse offerings include creating custom thesauri, building customized databases, organizing and publishing research results…even providing videos.

For more information about the NASA STI Program Office, see the following:

- Access the NASA STI Program Home Page at ***http://www.sti.nasa.gov***

- E-mail your question via the Internet to help@sti.nasa.gov

- Fax your question to the NASA Access Help Desk at (301) 621–0134

- Telephone the NASA Access Help Desk at (301) 621–0390

- Write to:
  NASA Access Help Desk
  NASA Center for AeroSpace Information
  7121 Standard Drive
  Hanover, MD 21076–1320
  (301)621–0390

NASA/TM—2004–213175

Analytical Modeling and Test Correlation of Variable Density Multilayer Insulation for Cryogenic Storage

L.J. Hastings
Alpha Technology, Inc., Huntsville, Alabama

A. Hedayat and T.M. Brown
Marshall Space Flight Center, Marshall Space Flight Center, Alabama

National Aeronautics and
Space Administration

Marshall Space Flight Center • MSFC, Alabama 35812

May 2004

TRADEMARKS

Trade names and trademarks are used in this report for identification only. This usage does not constitute an official endorsement, either expressed or implied, by the National Aeronautics and Space Administration.

Available from:

NASA Center for AeroSpace Information
7121 Standard Drive
Hanover, MD 21076–1320
(301) 621–0390

National Technical Information Service
5285 Port Royal Road
Springfield, VA 22161
(703) 487–4650

TABLE OF CONTENTS

1. INTRODUCTION 1

2. TEST ARTICLE ELEMENTS 3

2.1 Multipurpose Hydrogen Test Bed Tank 3
2.2 Environmental Shroud 4
2.3 Crogenic Insulation Subsystem 5
2.4 Instrumentation 10
2.5 Test Facility and Procedures 14

3. TEST RESULTS 18

3.1 Ground-Hold and Ascent Flight Simulations 18
3.2 Orbit-Hold Simulations 18

4. ANALYTICAL MODELS 21

4.1 Layer-by-Layer Model 21
4.2 Modified Lockheed Model 23
4.3 Computational Procedures 25

5. ANALYTICAL RESULTS 29

5.1 Modeling Comparisons and Test Data Correlations 29
5.2 Application Examples 30

6. CONCLUSIONS AND RECOMMENDATIONS 33

REFERENCES 35

LIST OF FIGURES

1. MHTB test tank and supporting hardware schematic 4
2. MHTB environmental shroud assembly 5
3. MHTB insulation concept—VD-MLI with foam substrate 6
4. Roll-wrapping application of VD-MLI and Dacron net spacing material 8
5. Top dome VD-MLI blanket assembly 8
6. Top dome VD-MLI blanket installation—beginning 9
7. Top dome VD-MLI blanket installation—complete 10
8. MHTB temperature measurement positions—top view 11
9. MHTB temperature measurement positions—side view 12
10. MHTB temperature measurement positions—bottom view 13
11. Representative MLI instrumentation profile on MHTB 14
12. MSFC east test area thermal vacuum facility, test stand 300 15
13. MHTB and test stand 300 facility simplified flow schematic 15
14. MHTB installation in test stand 300 vacuum chamber—beginning 16
15. MHTB installation in test stand 300 vacuum chamber—in chamber 16
16. MHTB TCS steady-state orbit-hold measured performance 19
17. Representative VD-MLI cross section 21
18. VD-MLI numerical model layout 26
19. Schematic of foam/VD-MLI system 28

LIST OF FIGURES (Continued)

20. Heat leak modeling correlations with test data, 45 layers VD-MLI 29

21. Heat leak predictions for 30 layers VD-MLI 30

22. Heat leak predictions for 60 layers VD-MLI 31

23. Heat leak predictions for 75 layers VD-MLI 31

LIST OF TABLES

1. VD-MLI properties and geometric variables 7

2. Insulation weight breakdown—MHTB and flight application 7

3. Measured VD-MLI thermal performance during on-orbit simulations 19

4. Variable density and standard MLI application comparison 32

LIST OF ACRONYMS AND SYMBOLS

ASME	American Society of Mechanical Engineers
CFM	cryogenic fluid management
DAM	double-aluminized Mylar
GN_2	gaseous nitrogen
LH_2	liquid hydrogen
MHTB	multipurpose hydrogen test bed
MLI	multilayer insulation
MSFC	Marshall Space Flight Center
SLPM	standard liters per minute
SOFI	spray-on foam insulation
VD-MLI	variable density multilayer insulation

NOMENCLATURE

A	empirical coefficient
C_2	an empirical constant
DX	actual thickness of separator between reflectors
f	relative density of the separator compared to solid material
K_n	Knudsen number
k	separator material conductivity
k_f	conductivity of the foam
k_g	gas conductivity
M	molecular weight of gas
N	total number of layers
N^*	layer density
N_s	number of radiative shields
n	(subscript) layer of interest
P	gas pressure
$P(x,T)$	pressure within the insulation as a function of position and local temperature
q_{total}	total heat transfer
R	gas constant
R_i	resistance between layer i–1 and layer i
T	temperature
T_C	temperature of the cold boundary
T_H	temperature of hot boundary
T_m	average temperature of hot and cold boundaries
α	accomodation coefficient
β	empirical parameter
ΔX	foam thickness
ε	emissivity of radiation shields
ε_C	emissivities of cold surfaces
ε_H	emissivities of warm surfaces
γ	specific heat ratio
σ	Stefan-Boltzmann constant

TECHNICAL MEMORANDUM

ANALYTICAL MODELING AND TEST CORRELATION OF VARIABLE DENSITY MULTILAYER INSULATION FOR CRYOGENIC STORAGE

1. INTRODUCTION

Future space programs and missions require efficient delivery of large payloads over great distances, necessitating the use of high-energy cryogenic upper stages. Therefore, cryogenic fluid management (CFM), including efficient and reliable insulation materials, is a crucial part of future space exploration. Insulation is a key element in long-duration missions requiring cryogenic storage since relatively small heat fluxes can result in significant boiloff losses, increased tank pressure, and increased liquid saturation conditions.

Multilayer insulations (MLIs) for cryogenic storage are designed for high vacuum conditions and typically consist of many radiation shields, separated by low conductivity spacer material, between the hot and cold boundaries. The radiation shielding normally consists of a thin plastic film coated on one or both sides with a thin layer of high reflectance metal, usually aluminum or gold. A detailed review of MLI is provided by Tein and Cunnigton.[1] MLI systems are often comprised of multiple double-aluminized Mylar® (DAM) radiation shields with Dacron® net spacer material between shields. While radiation generally dominates heat transfer, solid conduction through the spacer material becomes an issue at low temperatures such as those experienced by the inner MLI layers on a cryogenic fluid tank. To optimize the MLI for a cryogenic application, the colder inner layers can be spaced further apart than the warm outer layers where radiation dominates heat transfer. This type of MLI is referred to as variable density MLI (VD-MLI) because the layer spacing varies across the MLI cross section, reducing both insulation mass and thermal heat leak. The spacing geometry in a VD-MLI system can be controlled by the addition of bumper strips constructed with folded Dacron netting. The bumper strip thickness can be easily adjusted by varying the number of folds. In addition, larger but fewer perforations for venting during ascent to orbit can be used to reduce radiation heat transfer through the MLI.

MLI systems are suitable for low-pressure environments, whereas, at higher pressures simple foam insulation easily outperforms MLI. Thus, hybrid insulation concepts—combining foam insulation for atmospheric heat transfer protection (ground hold and launch) and MLI for optimum resistance during orbital space flight—have often been proposed in Earth-based upper-stage studies. However, virtually no large-scale hardware experience with foam/MLI concepts existed prior to 1990; therefore, foam insulation in combination with VD-MLI was selected for large-scale testing. Ultimately, the foam/VD-MLI combination was installed on and tested using the multipurpose hydrogen test bed (MHTB) at Marshall Space Flight Center (MSFC). Details regarding the test setup and results are reported by Martin and Hastings.[2] The primary purpose of this Technical Memorandum is to facilitate extension

of the VD-MLI concept (with the larger perforations in the radiation shielding) to other applications by describing the analytical modeling techniques, comparing the modeling with test results, and presenting some application examples.

2. TEST ARTICLE ELEMENTS

The major test article elements consist of the MHTB tank, an environmental shroud, cryogenic insulation subsystem, and test article instrumentation. Technical descriptions of each of these elements are summarized in sections 2.1 through 2.5, with further details presented in reference 2.

2.1 Multipurpose Hydrogen Test Bed Tank

The MHTB 5083 aluminum tank is cylindrical in shape with both a height and diameter of 3.05 m (10 ft) and 2:1 elliptical domes, as shown in figure 1. The tank has an internal volume of 18.09 m^3 (639 ft^3) and a surface area of 34.75 m^2 (374 ft^2), with a resultant volume-to-surface area ratio of 1.92 1/m (0.58 1/ft) that is reasonably representative of a full-scale vehicle liquid hydrogen (LH_2) tank. The tank is ASME pressure vessel coded for a maximum operational pressure of 344 kPa (50 psid) and was designed to accommodate various CFM technology and advanced concepts as updated versions become available. Major accommodations include a 60.9-cm- (24-in-) diameter manhole; pressurization and vent ports; fill/drain line (through tank top); 15.24- and 7.5-cm (6- and 3-in) general purpose penetrations with flanges on top; the zero-gravity pressure control subsystem (thermodynamic vent subsystem) penetration provisions on the tank bottom (one each 5.08-, 3.81-, and 1.27-cm tube) and an enclosure external to the tank; a 7.62-cm- (3-in-) diameter drain at the tank bottom for future growth; a continuous liquid level capacitance probe; two vertical temperature rakes; wall temperature measurements at selected locations; ullage pressure sensors; pressure control/relief safety provisions; internal mounting brackets for future equipment and structural “hard points” for temporary scaffolding and ladder; and low heat leak composite structural supports. Each of the penetrations is equipped with an LH_2 heat guard to intercept heat leak, thereby enabling more accurate measurement of the tank insulation performance.

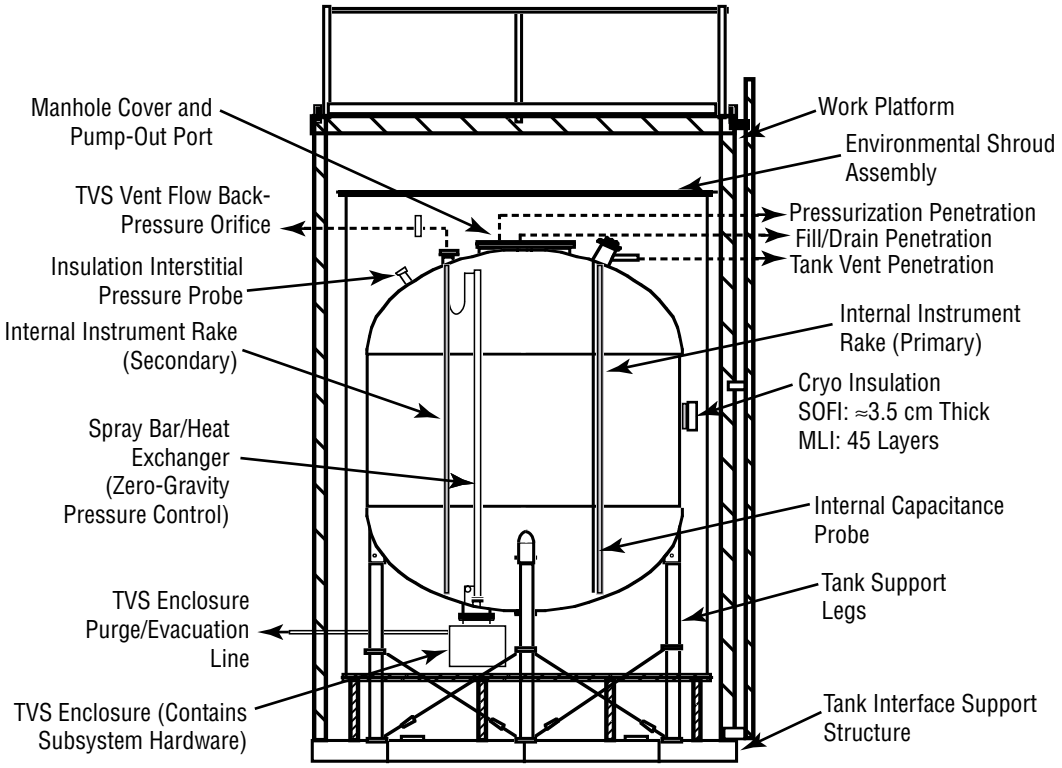

Figure 1. MHTB test tank and supporting hardware schematic.

2.2 Environmental Shroud

The MHTB tank is enclosed within an environmental shroud that simulates a ground-hold conditioning purge, similar to that in a payload bay, and enables the imposition of a range of uniform temperatures on the MLI external surfaces. The shroud (fig. 2) is 4.57 m (15 ft) high by 3.65 m (12 ft) in diameter, and contains a purge ring for distributing dry N_2. The shroud heater strips/cooling loops can impose either constant or time-dependent boundary temperatures ranging from 80 K (144 °R) to 320 K (576 °R) on the MHTB exterior surfaces.

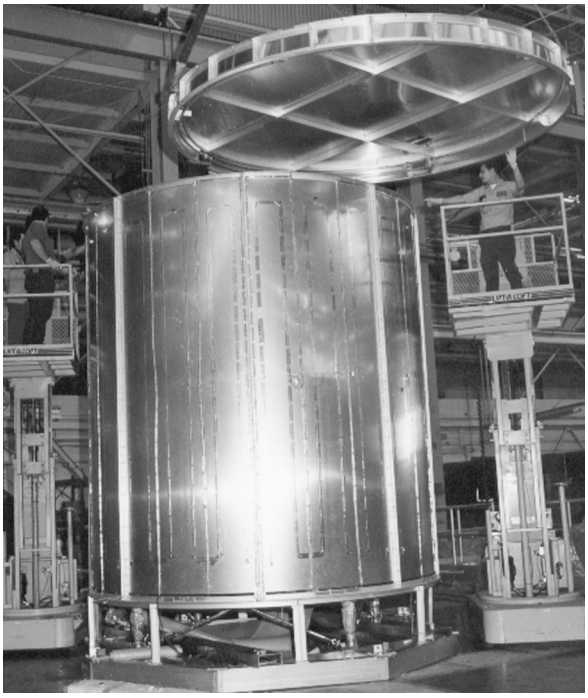

Figure 2. MHTB environmental shroud assembly.

2.3 Cryogenic Insulation Subsystem

As mentioned earlier, the MHTB insulation concept consists of a foam/VD-MLI combination. During ground hold and ascent flight, the foam element enables a gaseous nitrogen (GN_2) purge, as opposed to a helium purge, and reduces heat leak. The spray-on foam insulation (SOFI), termed Isofoam SS–1171, was applied directly to the tank surface with a robotic process at a thickness of 3.18 ± 0.63 cm (1.25 ± 0.25 in), which was the minimum that could be applied with available equipment and procedures. An average thickness of 3.53 cm (1.4 in) was calculated based on measurements with a Kaman eddy current device. In an actual application, only 1.4 cm (0.56 in) of foam would be required to avoid nitrogen liquefaction. Hand-sprayed insulation was applied in localized areas around some of the penetrations.

A 45-layer VD-MLI blanket placed over the SOFI provides thermal protection while at vacuum or orbital conditions. The blanket is composed of 1/2-mil DAM radiation shielding which is separated by a combination of B4A Dacron netting and B2A bumper strips (1/4-mil Mylar would be used in an actual application, but could not be obtained for this test without incurring a substantial DAM material cost increase). Unique features of the VD-MLI concept include utilization of a variable density (layers-per-unit thickness) concept for the radiation shields to provide a more weight-efficient insulation system and the use of fewer but larger perforations for venting during ascent to orbit. As illustrated in figure 3, the variable density was accomplished using bumper strips of variable thickness to provide more layers in warmer regions (16 layers/cm on outside segment), and fewer layers in the colder region where radiation blockage is less important (8 layers/cm). The layup resulted in an estimated average layer density of 12 layers/cm (30 layers/in). The vent hole perforation pattern, which provides a 2-percent open area,

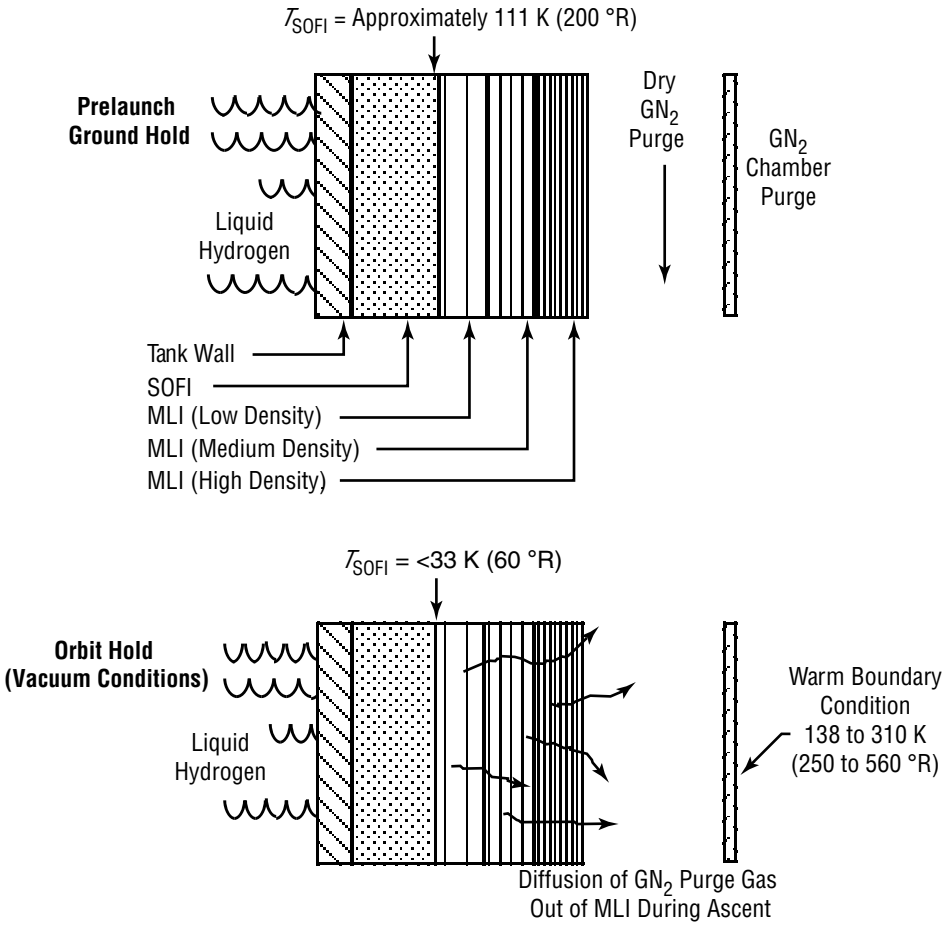

SOFI	Isofoam SS–1171, 3.53-cm Average Thickness		
MLI	45 Layers		
	Low-Density Layers 1 to 10	6 Bumper Strips	(≈8 Layers/cm)
	Medium-Density Layers 11 to 25	4 Bumper Strips	(≈12 Layers/cm)
	High-Density Layers 26 to 45	2 Bumper Strips	(≈16 Layers/cm)

Figure 3. MHTB insulation concept—VD-MLI with foam substrate.

is unusual in that the perforation size is large (1.27-cm (0.5-in) diameter) and the holes are more widely spaced (7.6 cm (3 in)). Standard perforations are 0.16- to 0.08-cm (0.063- to 0.031-in) diameter with about a 0.95-cm (0.37-in) spacing and 2–4 percent open area. The larger holes reduce the radiation view factor—hence, the radiation exchange—between layers. Additionally, the virtually seamless insulation enabled by the VD-MLI roll-wrap installation technique further reduces heat leak.

The insulation material weight properties and applied insulation weights are presented in tables 1 and 2, respectively. The foam and VD-MLI element weights totaled 45 and 33 kg (100 and 72 lb), respectively. However, the insulation weights in an actual application would be less with 1/4-mil aluminized Mylar and the foam thickness reduced to 1.4 cm (0.56 in). The applied foam and VD-MLI weights in a flight application with the same geometry as the MHTB tank would be 24 kg (54 lb) and 18 kg (40 lb), respectively, for a total of 42 kg (94 lb).

Table 1. VD-MLI properties and geometric variables.

Variable	Property
Foam conductivity, k_f	0.000866 (W/m-K)
Foam emissivity	0.80
MLI emissivity	0.03
MLI perforation factor	1.15
Shroud/surroundings emissivity	0.04
Interstitial gas	N_2
Interstitial gas molecular mass	0.028 (kg/mol)
Interstitial gas pressure	1.33×10^{-5} (Pa)
Accommodation coefficient	0.8
Interstitial gas specific heat ratio	1.4
Empirical spacer conduction coefficient	0.008
Separator material density	1,390 (kg/m^3)
Separator density/material density	0.0087

Table 2. Insulation weight breakdown—MHTB and flight application.

MHTB Application	Flight Application—Same Tank
Insulation Geometry • SOFI applied at avg. thickness of 3.56 cm (1.4 in) • 45 layers of 1/2-mil aluminized Mylar • 45 layers of Dacron netting • 1,219 m (4,000 ft) of aluminized tape • Bumpers – 533 m (1,750 ft) of 6 ply, layers 1 to 10 – 721 m (2,365 ft) of 4 ply, layers 11 to 25 – 1,073 m (3,520 ft) of 2 ply, layers 26 to 45	Insulation Geometry • SOFI avg. thickness of 1.78 cm (0.7 in) • 45 layers of 1/4-mil aluminized Mylar • Other MLI components same as MHTB
Applied Insulation Weight • MLI system weight = 32.68 kg (72 lb) – 1.36 kg (3 lb Dacron bumpers) – 2.72 kg (6 lb) aluminized tape – 12 kg (26.5 lb) Dacron netting – 16.6 kg (36.5 lb) aluminized Mylar • SOFI system weight = 45.36 kg (100 lb)	Applied Insulation Weight • MLI system weight = 24.4 kg (53.8 lb) – 8.4 kg (18.3 lb) aluminized mylar – Other components same as MHTB • SOFI system weight = 18.14 kg (40 lb)

A commercial roll-wrapping technique was utilized for the barrel section application wherein the DAM, B4A Dacron net spacer, and B2A Dacron bumper materials were rolled on simultaneously (fig. 4). The dome insulation was prefabricated on a flat table (fig. 5); then, about six layers were temporarily taped to a holding fixture (handmade from lightweight plastic piping material). The holding fixture was then positioned by one person against the dome while two other people installed the MLI layer by layer using Mylar tape and interleaving each dome layer with the corresponding barrel blanket layer (fig. 6). The dome/barrel section layers were overlapped by ≈25 cm (10 in); the completed upper dome blanket installation is shown in figure 7. Using the preceding VD-MLI installation techniques on a 3-m-diameter tank set (hydrogen and oxygen) would result in an estimated savings of 2,400 man-hours. Further details regarding the insulation material and installation techniques are presented in reference 2.

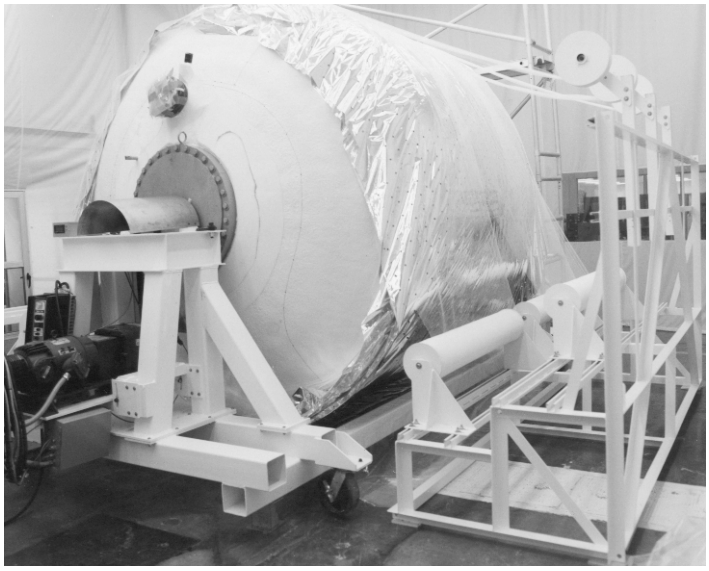

Figure 4. Roll-wrapping application of VD-MLI and Dacron net spacing material.

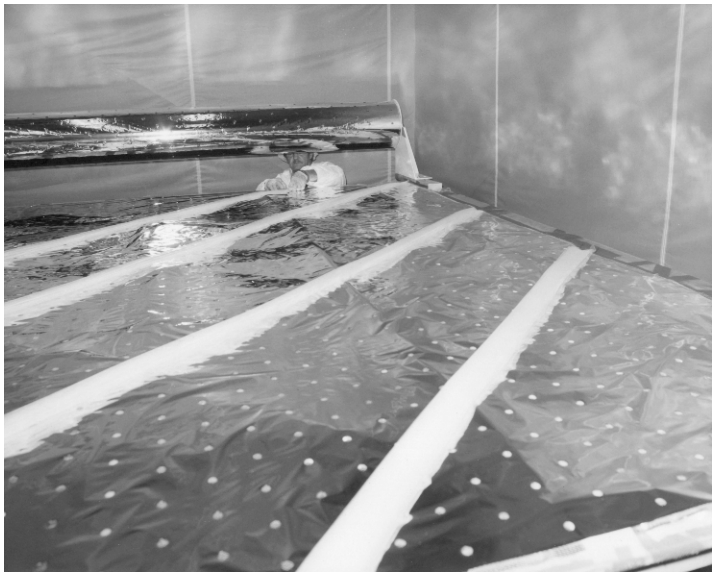

Figure 5. Top dome VD-MLI blanket assembly.

Figure 6. Top dome VD-MLI blanket installation—beginning.

Figure 7. Top dome VD-MLI blanket installation—complete.

2.4 Instrumentation

The test article and environmental shroud instrumentation details are presented in reference 2; however, the instrumentation arrangement is summarized herein. The test article instrumentation consists primarily of thermocouple and silicon diodes to measure insulation, fluid, and tank wall temperatures. The general instrumentation layout is illustrated in figures 8–10, which represent the top, front, and bottom views of the test tank without insulation for clarification. Typically, silicon diodes (Lakeshore type DT–470–11A) temperature transducers are positioned in areas of lowest temperatures because of higher accuracy as compared with thermocouples. As illustrated in figure 9, MLI temperature profiles or gradients are measured at seven positions with one silicon diode and four thermocouples (fig. 11) placed at each of the seven measurement positions. The MLI interstitial pressure is measured at the foam/VD-MLI interface and a sampling port for both dewpoint level and gas species is provided.

Two of the four composite legs, the vent, fill/drain, pressurization, pressure sensor probe, and manhole pump-out penetrations are instrumented to determine the solid conduction component of heat leak. The tank is internally equipped with two instrumentation rakes and a capacitance liquid level probe, all supported from the top of the tank. The rakes are equipped with silicon diodes attached at 22.9-cm (9-in) intervals. The instrumentation rakes provide temperature-gradient measurements within both ullage and liquid, in addition to providing a backup to the continuous liquid level capacitance probe.

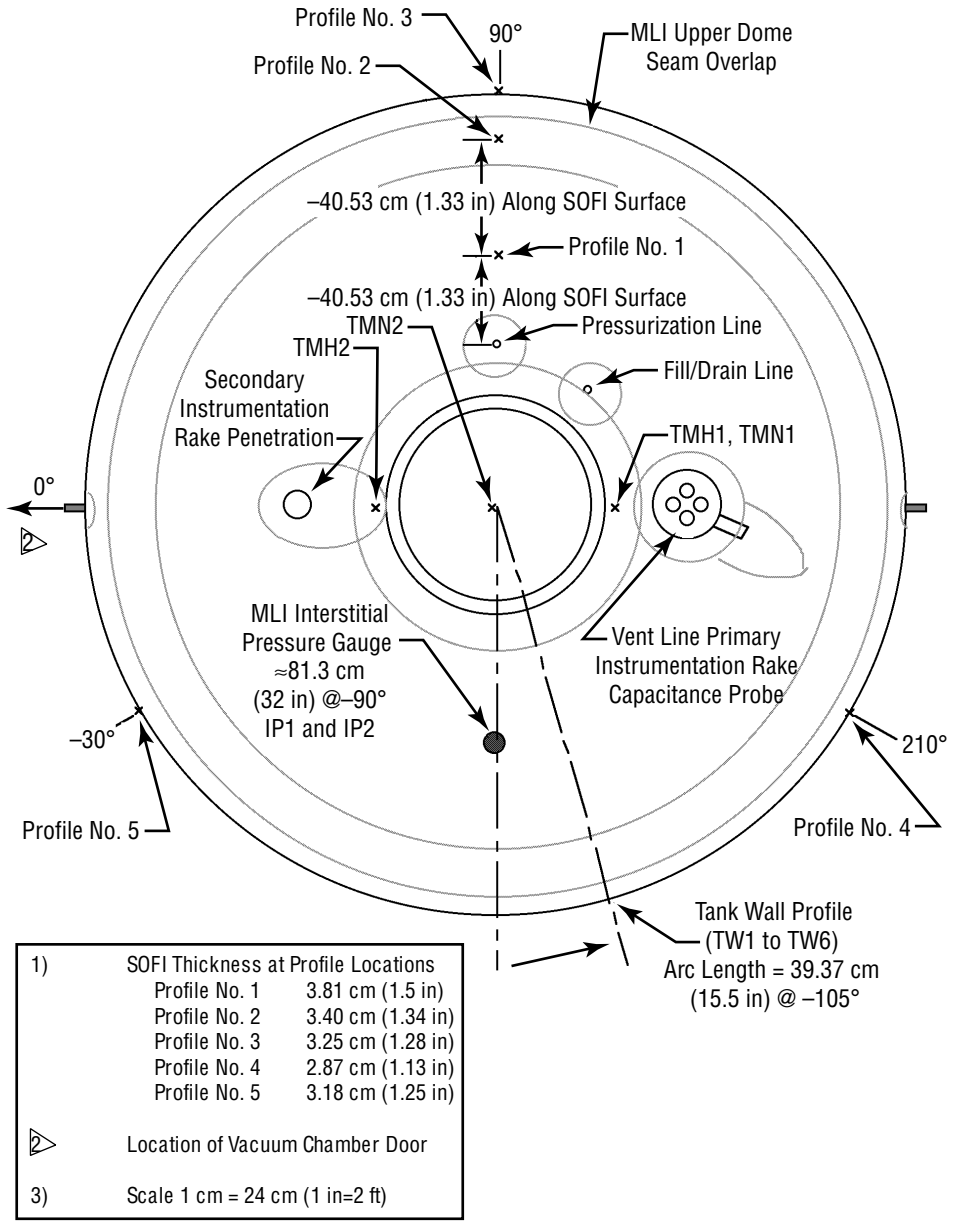

Figure 8. MHTB temperature measurement positions—top view.

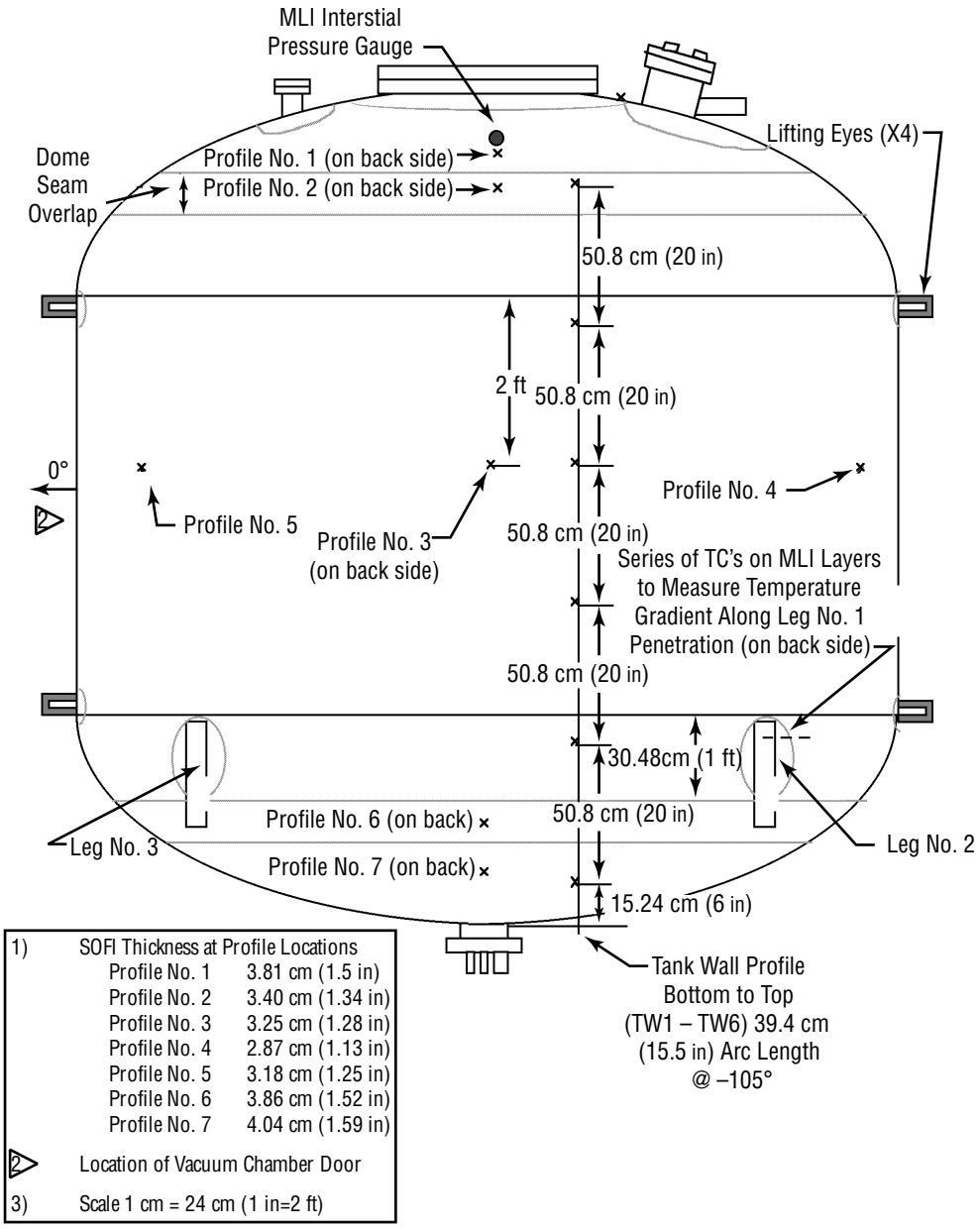

Figure 9. MHTB temperature measurement positions—side view.

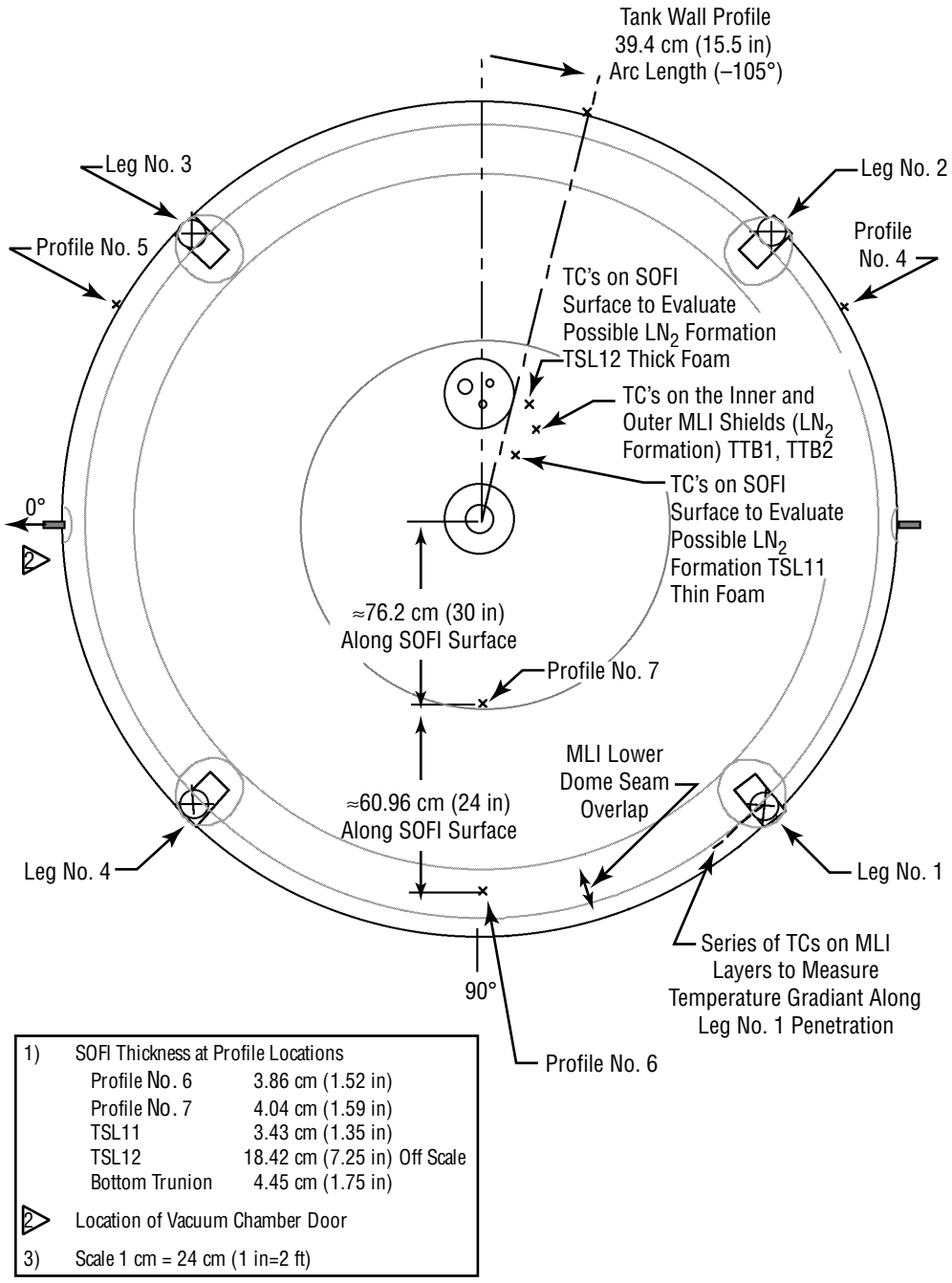

Figure 10. MHTB temperature measurement positions—bottom view.

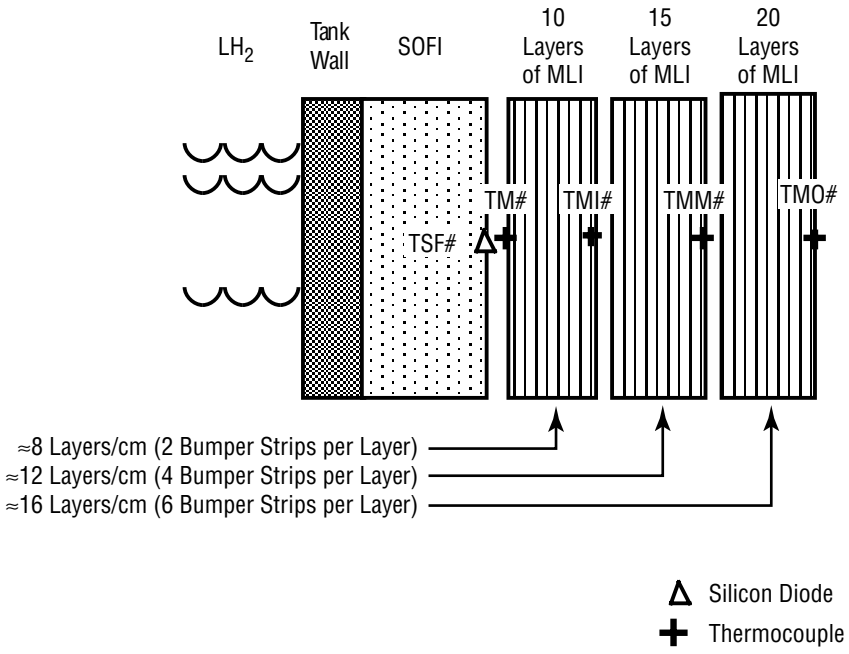

Figure 11. Representative MLI instrumentation profile on MHTB.

The environmental shroud is composed of 17 individual panels, each equipped with a minimum of two thermocouples attached to the inner surfaces and placed beneath the electrical heating strips. These thermocouples are used with a closed-loop control system to regulate the temperature of each shroud panel.

2.5 Test Facility and Procedures

Testing was performed at the MSFC east test area thermal vacuum facility, test stand 300 (fig. 12). The test article and facility flow schematic is presented in figure 13. The vacuum chamber is cylindrical and has usable internal dimensions of 5.5 m (18 ft) in diameter and 7.9 m (26 ft) in height. Personnel access is through a small side-entry door, but the chamber lid is removable for installation of large test articles (figs. 14 and 15). The chamber pumping train consists of a single-stage GN_2 ejector, three mechanical roughing pumps with blowers, and two 1.2-m- (48-in-) diameter oil diffusion pumps. Liquid nitrogen cold walls surround the usable chamber volume providing cryopumping and thermal conditioning, resulting in vacuum levels as low as 10^{-8} torr. The combination of test facility and test article shroud systems enable simulation of orbital vacuum and provide test article external surface temperatures ranging from 80 K to 320 K (140 °R to 576 °R).

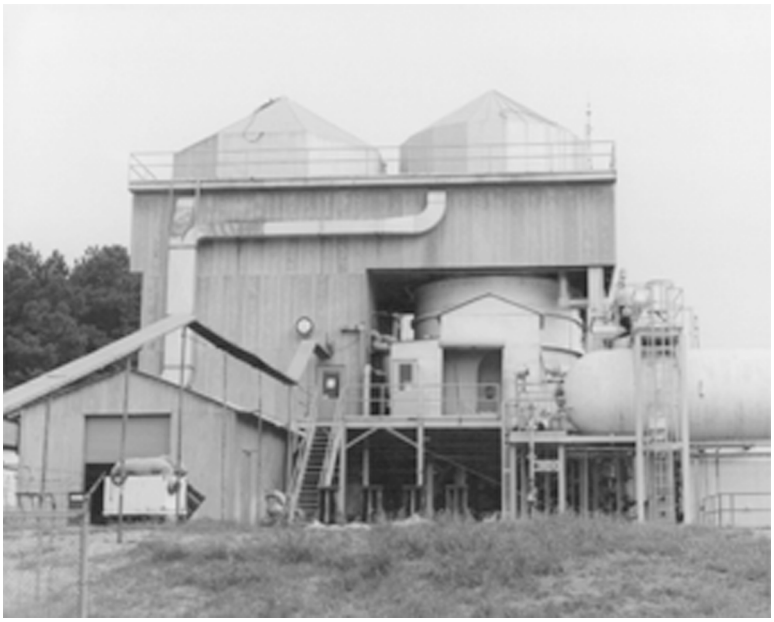

Figure 12. MSFC east test area thermal vacuum facility, test stand 300.

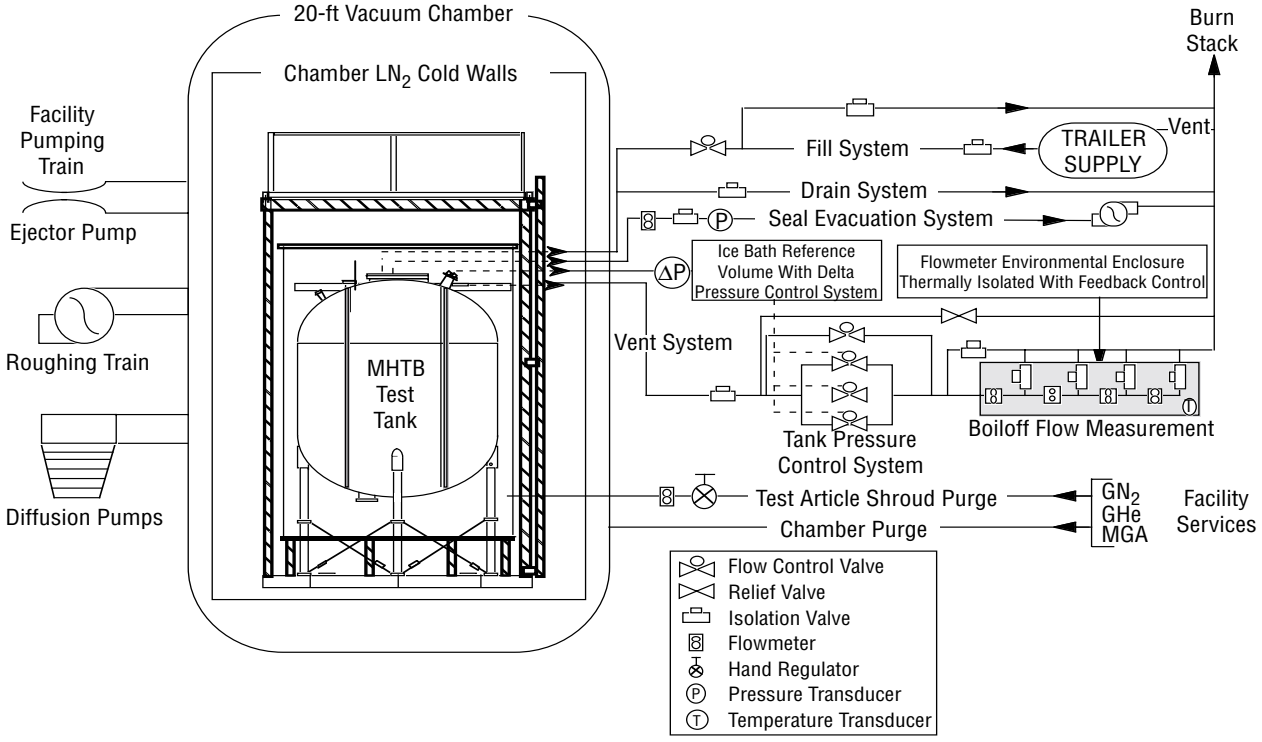

Figure 13. MHTB and test stand 300 facility simplified flow schematic.

Figure 14. MHTB installation in test stand 300 vacuum chamber—beginning.

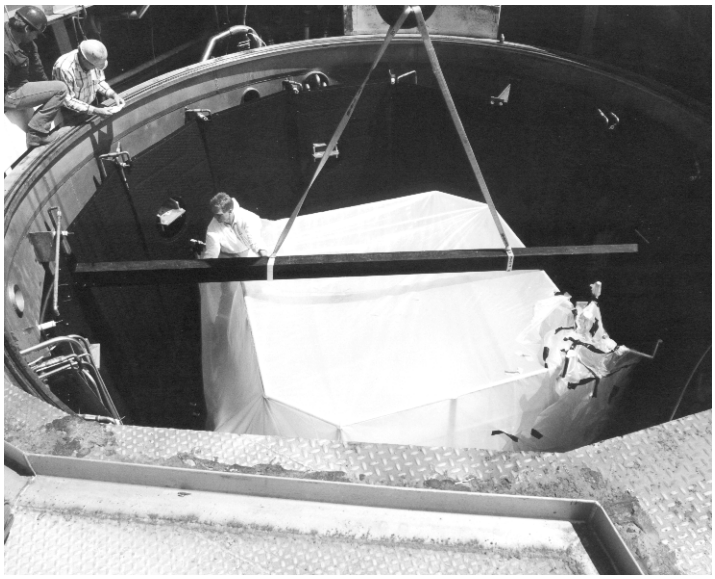

Figure 15. MHTB installation in test stand 300 vacuum chamber—in chamber.

During the orbital simulation phase of the heat leak testing, conditions within the MHTB were controlled utilizing the facility subsystems described below:

• A tank pressure control subsystem was used to maintain the MHTB ullage pressure at the required steady-state conditions. The system was composed of several flow control valves (located in the vent line), each of which was regulated through a closed-loop control system. This control loop manipulated the valve positions based on a comparison of the measured tank ullage pressure and the desired set point. The system successfully maintained set points ranging from 110 to 124 kPa (16–18 psia) with a tolerance of ±0.00689 kPa (±0.001 psi) for the orbital simulation conditions.

• Hydrogen boiloff flow instrumentation was located in the vent downstream of the flow control valves. During orbit-hold simulations, one of three mass flowmeters, each with a different range, was used. These meters spanned flow ranges of zero to 280 standard liters per minute (SLPM), zero to 50 SLPM, and zero to 1 SLPM with accuracies of ±0.8, ±1, and ±1 percent of full scale, respectively. To prevent ambient temperature effects on measurement accuracy, the flowmeter system was placed within a containment box and equipped with a temperature-controlled purge, which maintained the box interior at constant temperature, typically 306 K (550 °R).

Steady-state vacuum and thermal conditions—within both the chamber and MLI—were achieved before each on-orbit heat leak test phase. The four criteria that had to occur simultaneously for steady-state thermal conditions were as follows:

(1) Interstitial MLI pressures had to be 10^{-5} torr or less to preclude a transient convective heat transfer effect as the insulation pressure continues to drop. A vacuum chamber pressure of 10^{-6} torr or less was required to ensure an adequate vacuum within the insulation.

(2) Insulation temperatures (MLI and SOFI) had to be in a steady-state condition with the MLI exterior surface temperature at the prescribed setpoint imposed by the environmental shroud. Insulation equilibrium was assumed to exist once temperature transients of no more than 0.55 K in 6 hr was measured in any section of the insulation system.

(3) Thermal equilibrium of the LH_2 had to be maintained through precise ullage pressure control during the low heat leak, orbital simulation. Ullage pressure was maintained at a setpoint in the range of 110.316 to 124.106 kPa (16 to 18 psia) with a tolerance of 0.00689 kPa (0.001 psi).

(4) The vented ullage gas temperature had to increase with time (positive slope), indicating that the tank dome was in thermal equilibrium; i.e., the dome was no longer cooling and contributing to the vented gas enthalpy.

3. TEST RESULTS

Three ground-hold tests, two rapid ascent simulations, and three orbit-hold simulations were performed over a period of 10 mo to evaluate the MHTB insulation performance. Test results are summarized in sections 3.1 and 3.2 and further details are presented in reference 2.

3.1 Ground-Hold and Ascent Flight Simulations

Three tests were performed with MLI GN_2 purge temperatures ranging from 270 K to 290 K and resulted in heat leaks from 61 to 64 W/m^2 (2,119 to 2,224 W) which closely corresponded to the predicted 62.5 W/m^2 (2,172 W). The SOFI surface temperatures were maintained at or above 150 K and successfully prevented purge gas liquefaction. Additionally, GN_2 purged foam/MLI arrangement yielded a hydrogen density degradation of only 3 percent as compared to 13 percent with a helium-purged MLI (without foam) arrangement.

The rapid ascent simulations were conducted to evaluate the MLI structural integrity under broadside venting loads and the time required to achieve thermal equilibrium. Video camera observations during the rapid chamber evacuation (760 to 35 torr in ≈120 s) verified the structural robustness of the roll-wrapped, virtually seamless construction. Approximately 11,000 and 8,000 min were required to attain a steady-state heat leak in the first and second test series, respectively.

3.2 Orbit-Hold Simulations

Results from the three orbit-hold simulations, tabulated in table 3 and graphically presented in figure 16, were conducted with warm boundary temperatures ranging from 305 K to 164 K, with and without penetration heat guards, and with an off-nominal (damaged) MLI configuration in the last test series. The first test series (P9502), conducted without heat guards, yielded an insulation heat leak (total heat leak minus penetration heat leak) of 0.28 W/m^2 (9.75 W) with the warm boundary at 305 K. The three separate tests in the second test series (P9601) each yielded an insulation heat leak of 0.22 W/m^2 with the 305 K boundary. The lower heat leak observed in the second series is attributed to reduced out-gassing, probably from the foam insulation. The total heat leak during the P9601 test series with the 305 K boundary and deactivated heat guards ranged from 10.9 to 11.07 W; whereas, 7.89 W, occurred with the penetration heat guards activated. The insulation heat leak of 0.22 W/m^2 (7.63 W) with the heat guards on, most closely represents the true insulation performance at the 305 K boundary condition. The penetration heat leaks presented in table 1 are based on the difference between the measured total heat leak without heat guards and the total heat leak with heat guards during series P9601, and averaged 3.35 W at the 305 K boundary condition. With the 164 K boundary, the insulation heat leak was 0.11 and 0.08 W/m^2 (3.95 and 2.89 W) during series 9502 and 9601, respectively.

Table 3. Measured VD-MLI thermal performance during on-orbit simulations.

Measured Heat Leak Elements					
Series	Boundary *T* (K)	Total (W)	Penetration (W)	Insulation (W)	Insulation (W/m^2)
1st P9502	305	13.10	3.35	9.75	0.28
2nd P9601	305	11.07	3.35	7.72	0.22
2nd P9601	305	7.89	0.26	7.63	0.22[a]
2nd P9601	305	10.90	3.35	7.55	0.22
3rd P9602A	305	12.87	3.35	9.50	0.27[b]
3rd P9602A	305	12.11	3.35	8.76	0.25[b]
3rd P9602A	235	8.41	2.19	6.22	0.18[b]
3rd P9602A	235	7.28	1.89	5.39	0.16[b]
1st P9502	164	5.34	1.39	3.95	0.11
2nd P9601	164	3.90	1.01	2.89	0.08

[a]Penetration heat guards activated
[b]Top dome insulation damaged before test

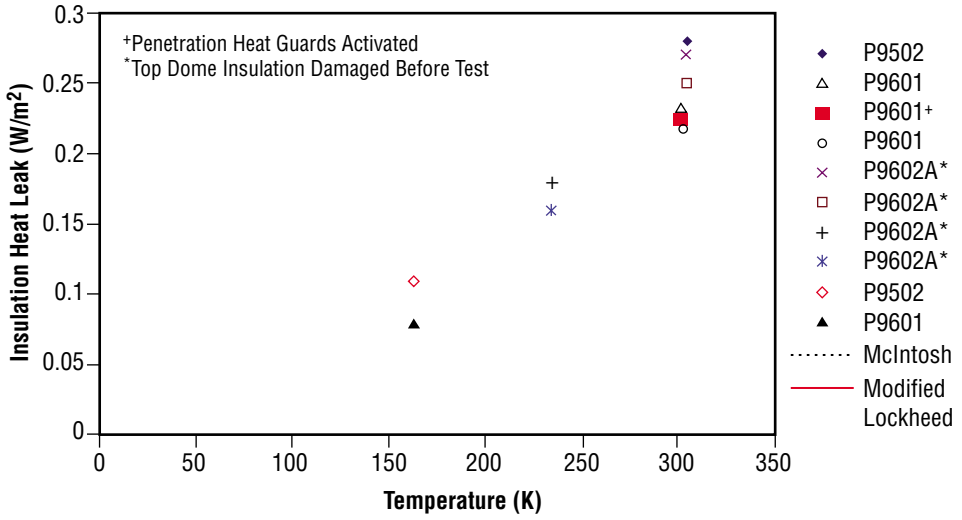

Figure 16. MHTB TCS steady-state orbit-hold measured performance.

Results from the third test series (P9602A) were compromised by significant MLI damage that occurred after the second series (P9601). During a pressurized liquid expulsion test, the manhole cover seal developed a leak that overpressured and tore the manhole MLI (≈1.5 m^2). The outer DAM layer was also torn loose, exposing ≈11 m^2 of Dacron on the tank top and sidewall. Even with the damaged insulation, the measured boiloff rates of 10.47 to 10.93 W (with the 305 K boundary) clearly demonstrate thermal control subsystem robustness. Additionally, a 235 K boundary was imposed in the third series and produced insulation heat leaks of 0.18 to 0.16 W/m^2 (6.22 to 5.39 W).

Historically, MLI performance has been expressed in terms of percent boiloff per day versus tank volume. With the MHTB 45-layer blanket and warm boundary condition (305 K), a boiloff loss of

0.117 percent per day was measured with no penetration heat leak. McDonnell Douglas set the standard for demonstrated MLI performance in 1973 (ref. 3). A boiloff rate of 0.2 percent per day was achieved on a 2.67-m- (105-in-) diameter tank with 70 layers of DAM and no penetration heat leak. Therefore, the variable density MLI decreased boiloff relative to that with the standard MLI by 41 percent with 25 fewer layers.

4. ANALYTICAL MODELS

As mentioned earlier, MLIs typically consist of many radiation shields, separated by low thermal conductivity spacer material between the warm and cold boundaries. Figure 17 depicts a representative cross-sectional view of a VD-MLI layup arrangement. To facilitate extension of the MHTB-type insulation concept to other applications, analytical modeling techniques were developed for a VD-MLI combined with the larger and fewer vent holes and an optional SOFI substrate.[4] Two analytical models were investigated for predicting VD-MLI performance. The "layer-by-layer" model is based on a methodology developed by McIntosh,[5] and the other model is a modification of the "Lockheed model." The two analytical modeling approaches and computational procedures are discussed in subsequent sections.

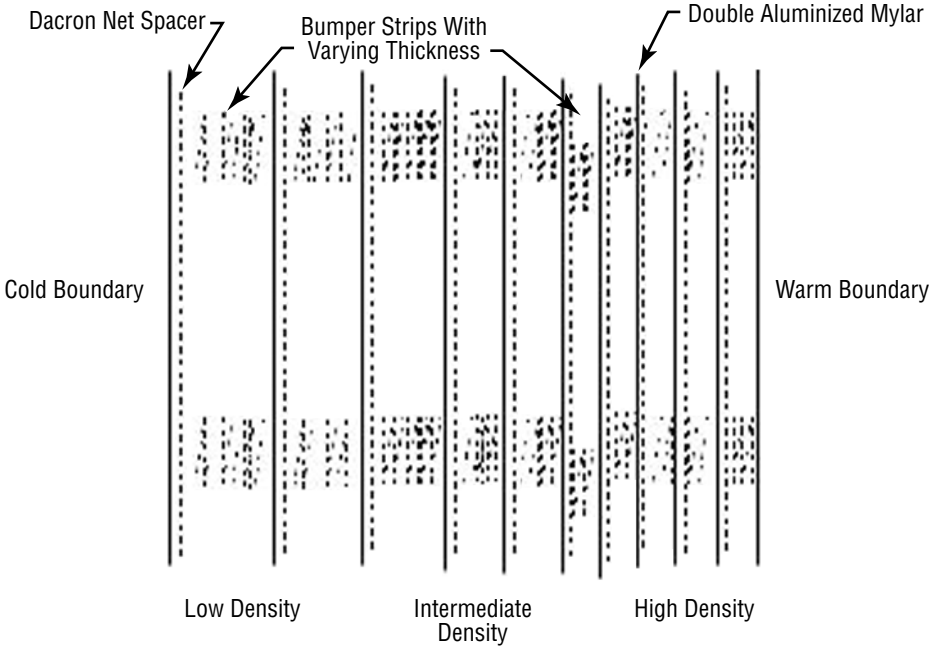

Figure 17. Representative VD-MLI cross section.

4.1 Layer-by-Layer Model

The McIntosh-based layer-by-layer model accounts for three modes of heat transfer: thermal radiation between shields, gas conduction, and solid conduction through the spacer or separator materials. The total heat flux through the MLI is given by

$$q_{\text{total}} = q_{\text{radiation}} + q_{\text{gas conduction}} + q_{\text{solid conduction}} \cdot \tag{1}$$

The radiation heat transfer is

$$q_{\text{radiation}} = \sigma (T_H^4 - T_C^4)/(1/\varepsilon_H + 1/\varepsilon_c - 1) \ , \tag{2}$$

where

σ = Stefan-Boltzmann constant = 5.675×10^{-8} W/m^2-K^4
T_H = temperature of warm surface, K
T_C = temperature of cold surface, K
ε_H = emissivities of warm surfaces
ε_C = emissivities of cold surfaces.

The gas conduction component is represented by the following:

$$q_{\text{gas conduction}} = C_1 \, P \, \alpha \, (T_H - T_C) \ , \tag{3}$$

where

$k_g = C_1 \, P \, \alpha$ = gas conduction, W/m^2-K
P = gas pressure, Pa
$C_1 = [(\gamma + 1)/(\gamma - 1)] \, [R/8 \, \pi \, M \, T]^{1/2}$
α = accommodation coefficient
$\gamma = C_p/C_v$
R = gas constant, 8.314 kJ/mol-K
M = molecular weight of gas, kg/mol
T = vacuum chamber exterior temperature, normally 300 K
C_1 = 1.1666 for air
C_1 = 2.0998 for helium.

Conduction through the solid is expressed as,

$$q_{\text{solid conduction}} = K_s \ (T_H - T_C) \ , \tag{4}$$

where

$K_s = C_2 \, f \, k/DX$
C_2 = an empirical constant = 0.008 for Dacron netting
f = relative density of the separator compared to solid material
k = separator material conductivity, W/m-K
DX = actual thickness of separator between reflectors, m.

Curve-fit equations have been applied to express thermal conductivity for Dacron, silk net, and glass paper separator materials as a function of temperature (T). For Dacron, the following equation is provided:

$$k = 0.017 + 7\times10^{-6}*(800 - \text{T}) + 0.0228 \ln(T) \ . \tag{5}$$

4.2 Modified Lockheed Model

Like the layer-by-layer method, three heat transfer mechanisms are considered with the Lockheed model—solid conduction, gas conduction, and radiation between shields. A semiempirical expression is developed and used to approximate the variation of conductance with temperature in terms of conductivity, modulus of elasticity, and Poisson's ratio of spacer material.

The solid conductive heat transfer with a nonlinear dependency of thermal conductivity of the spacer fibers is described as

$$q_{\text{solid conduction}} = \mathrm{A}(N^*)^n \, T_m \, (T_H - T_C)/N_s \ , \tag{6}$$

where

A = empirical coefficient
N^* = layer density
T_m = average temperature of hot and cold boundaries ($T_m = (T_H + T_C)/2$)
T_H = temperature of hot boundary
T_C = temperature of cold boundary
N_s = number of radiative shields.

The gas conductive heat transfer under free-molecule conditions (Knudsen number, $K_n > 10$), is shown as

$$q_{\text{gas conduction}} = \beta \, (\gamma + 1/\gamma - 1)/(R/8 \, \pi \, M \, T_m)0.5 \, P \, (T_H - T_C) \ , \tag{7}$$

where

P = pressure, torr
T = temperature, K
M = molecular weight
γ = specific heat ratio
β = empirical parameter.

The radiative heat transfer between the perforated shields is given by

$$q_{\text{radiation}} = \mathrm{B} \, \varepsilon \, \sigma \, (T_H{}^{4.67} - T_C{}^{4.67})/N_s \ , \tag{8}$$

where

ε = emissivity of the shields
B = empirical parameter.

The total heat transfer can then be expressed as

$$q_{\text{total}} = q_{\text{solid conduction}} + q_{\text{radiation}} + q_{\text{gas conduction}} \tag{9}$$

$$q_{\text{total}} = \text{A}\,(N^*)^n\,T_m\,(T_H - T_C)/N_s + \text{B}\,\sigma\,(T_H^{4.67} - T_C^{4.67})/N_s$$

$$+ \text{C}\,P(x,T)\,(T_H^{(m+1)} - T_C^{(m+1)}/N_{\text{s}}\ , \tag{10}$$

where

$P(x,T)$ = pressure within the insulation as a function of position and local temperature.

Coefficients A, B, and C as well as the exponents m and n are derived from the particular insulation system and intestial gas.

For perforated aluminized shields, nitrogen gas, and glass tissue spacer material, the suggested Lockheed equation for the total heat transfer becomes the following:

$$q_{\text{total}} = 7.30\times10^{-8}\,(N^*)^{2.63}\,T_m(T_H - T_C)/N_s + 7.07\times10^{-10}\,\varepsilon\,(T_H^{4.67} - T_C^{4.67})/N_s$$

$$+ 1.46\times10^{4}\,P\,(T_H^{0.52} - T_C^{0.52})/N_s\ , \tag{11}$$

where

q_{total} = total heat transfer, W/m^2
ε = 0.04
N^* = layers/cm.

In the original Lockheed equation, the radiation shield hole sizes and spacer material were different than those of the MHTB test article; therefore, the empirical parameters A and B had to be adjusted to accommodate the MHTB insulation. The coefficient A influences the conduction through the spacer material, which was Tissuglas in the Lockheed equation, while Dacron net was used in the test article. To modify the solid conduction term, the Dacron conductivity function provided by McIntosh has been incorporated into the conduction term. Thus, the following equation describes the effective conductivity K_{eff}:

$$K_{\text{eff}} = C_2\,f\,k = \text{A}\,T_m\ , \tag{12}$$

where

k = $(0.017 + 7\times10^{-6}(800 - T) + 0.0228\,\ln(T))$
C_2 = 0.008
f = 0.03.

The radiation coefficient B in the original Lockheed equation accounts for radiation heat transfer between the shields and was specified to represent shields perforated with 0.119-cm- (0.047-in-) diameter holes and a fractional open area (holes area/shield area) of 0.01. However, the perforated shields used in the MHTB MLI (hole diameter of 1.27 cm (0.5 in) and fractional open area of 0.02) necessitated

the selection of a new value for B. Based on empirical radiation heat flux curves for various hole sizes and open area ratios provided in reference 7, the adjusted value of B was calculated to be 4.944×10^{-10}.

Therefore, the "modified Lockheed" equation becomes the following:

$$q_{\text{total}} = 2.4\times10^{-4} *(0.017 + 7\times10^{-6}\,(800 - T) + 0.0228\,\ln(T))*\,(N^*)^{2.63}(T_H - T_C)/N_s$$

$$+ 4.944\times10^{-10}\varepsilon\,(T_H{}^{4.67} - T_C{}^{4.67})/N_s + 1.46\times10^{4}\,P\,(T_H{}^{0.52} - T_C{}^{0.52})/N_s\ . \qquad (13)$$

4.3 Computational Procedures

4.3.1 Layer-by-Layer Model

The total conductance between two adjacent MLI layers can be determined by adding the conductances of the three parallel heat transfer paths:

$$K_T = K_R + K_s + K_g\ , \qquad (14)$$

where

$K_R = [\sigma\,(T_H + T_C)(T_H{}^2 + T_C{}^2)]/(1/\varepsilon_H + 1/\varepsilon_c - 1)$
$K_s = C_2\,f\,[0.017 + 7\times10^{-6} *(800 - T) + 0.0228\,\ln(T)]/DX$
$K_g = C_1\,P\alpha.$

The total heat transfer resistance between two adjacent MLI layers is given by the reciprocal of the total conductance,

$$R_T = \frac{1}{K_T}\ , \qquad (15)$$

and is a third-order function of T_H and T_C.

Modeling the foam insulation between the tank wall and the first MLI layer is accomplished with a simplified solid conduction equation. The resistance of the foam insulation is

$$R_f = \frac{\Delta X_f}{k_f}\ , \qquad (16)$$

where

k_f = conductivity of the foam
ΔX = foam thickness.

The numerical scheme makes use of successive iterations to calculate a solution to the heat transfer equations. First, a linear temperature profile is assumed across the MLI layers; then, from the linear profile, individual layer heat transfer resistances are calculated. A new temperature profile is then calculated from the resistances based on the following:

$$T_n = T_c + \frac{R_f + \sum_{0}^{n} R_i}{R_f + \sum_{0}^{N+1} R_i} \quad , \tag{17}$$

where

R_i = resistance between layer *i–1* and layer *I*
N = total number of layers
n = (subscript) the layer of interest.

The heat flux is calculated from any layer resistance and its corresponding temperature drop:

$$q = \frac{(T_{n-1} - T_n)}{R_n} \quad . \tag{18}$$

This process is repeated until the difference between successive heat flux calculations are within a specified limit—user option. Figure 18 provides a pictorial representation of the VD-MLI model layout.

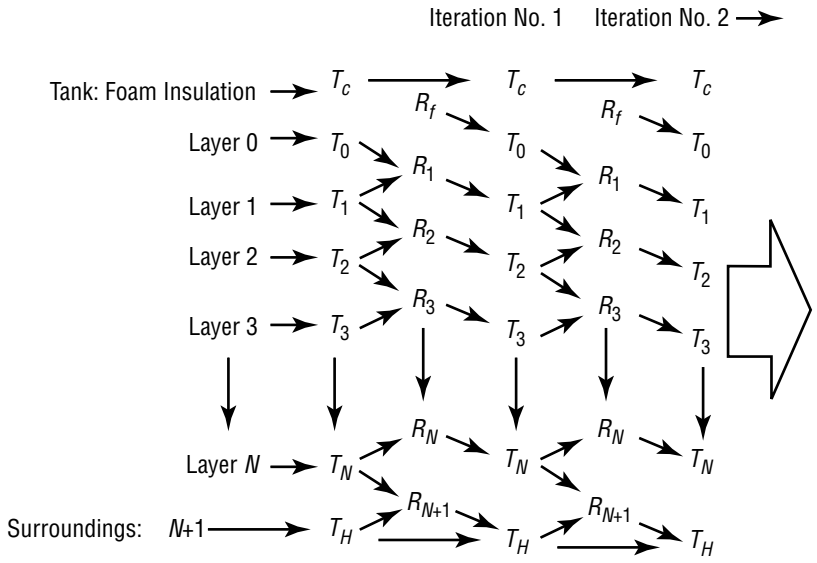

Figure 18. VD-MLI numerical model layout.

The MHTB foam/VD-MLI system is made up of a 3.53-cm-thick foam insulation layer, covered by 45 MLI layers. The 45 MLI layers are divided into three constant density blankets. The first blanket has 10 layers spaced at 8 layers/cm, the second blanket is made up of 15 layers spaced at 12 layers/cm, and the outermost or third blanket has 20 layers spaced at 16 layers/cm. The spacer material is Dacron netting, which for the entire blanket, occupies a volume of 1.105 m^3 and has a mass of 13.3 kg, resulting in a separator density of 12.03 kg/m^3. Other VD-MLI properties and geometric variables used by the model are provided in table 1.

In the layer-by-layer approach, the foam, each shield layer, and the shroud are considered to be separate nodes. Therefore, the foam/MLI system model is comprised of 47 nodes. The foam element is optional and can be removed from the computational process by setting the foam thickness input to near zero.

4.3.2 Modified Lockheed Equation

Figure 19 represents a foam/MLI combination with five different segments. The first segment is the foam with a conductivity, k_f, of 0.00083 W/m-K and a thickness of 3.53 cm. The second, third, and fourth segments represent the three segments of MLI with different layer densities and number of shields. The layer density, N*, and number of shields for MLI segments 1 through 3 are 8, 12, and 16 layers/cm, and 10, 15, and 20 shields, respectively. Finally, the last segment is considered to be the shroud with an emissivity of 0.04. Therefore, the heat transfer model elements consist of conduction through the foam, three segments of MLI using the Lockheed equation for each segment, and radiation exchange between the shroud and the last MLI shield. The cold temperature boundary condition at the interior of the foam and hot temperature at the exterior of the shroud describe the cryogenic liquid and the environment temperature, respectively. At steady-state conditions, the following relations can be written as

$$q_{\text{foam}} = q_{\text{layer1}} = q_{\text{layer2}} = q_{\text{layer3}} = q_{\text{shroud}} \quad . \tag{19}$$

The q's, T_1, T_2, and T_3 are unknowns. Using equation (19), a system of four equations with four unknowns can be developed. Because of the radiation terms, this system of equations is nonlinear and is solved iteratively. First, for prescribed cold and hot boundary temperatures, initial MLI segment interface temperatures are assigned and the heat rate through each segment is calculated. Then, using the heat rate and guessed temperature, the resistance of each segment is computed. The new heat rate and resistance of each segment can then be used to compute new temperatures. The process is repeated until the solution converges. The convergence of the solutions implies that the total heat transfer rate through each segment is the same and the temperature of each MLI segment interface for two consecutive iterative steps becomes equal within an allowable difference. As with the layer-by-layer model, the foam element is optional.

Figure 19. Schematic of foam/VD-MLI system.

5. ANALYTICAL RESULTS

5.1 Modeling Comparisons and Test Data Correlations

Comparisons of the two analytical modeling techniques for the 45-layer MHTB VD-MLI/foam combination and correlations with measured (MHTB) data are presented in figure 20. The measured data included hot boundary temperatures of 164 K, 235 K, and 305 K with a cold boundary temperature of 20 K. With the 305 K warm boundary condition, the insulation heat leak values predicted with the layer-by-layer model and modified Lockheed equation are within 5 and 8 percent of the measured data, respectively. With the 235 K boundary, it is believed that the measured heat leak is above that predicted, primarily because that particular test series (P9062A) was conducted with damaged insulation. With the 164 K warm boundary, the modified Lockheed model and layer-by-layer predictions are 30 and 34 percent below the measured data, respectively. The lack of correlation at the lower temperature boundary condition is attributed to a "lower than actual" effective thermal conductivity computed by the models. Apparently, the relative errors in the empirical computations of radiation and conduction effects compensate such that the correlation with the test data is relatively good at higher boundary temperatures; whereas, the conductivity term dominates at the lower temperatures and the deviation is manifested. However, the practical effect of the deviation is not significant since the heat leak magnitude at 164 K is relatively small (<0.1 W/m^2).

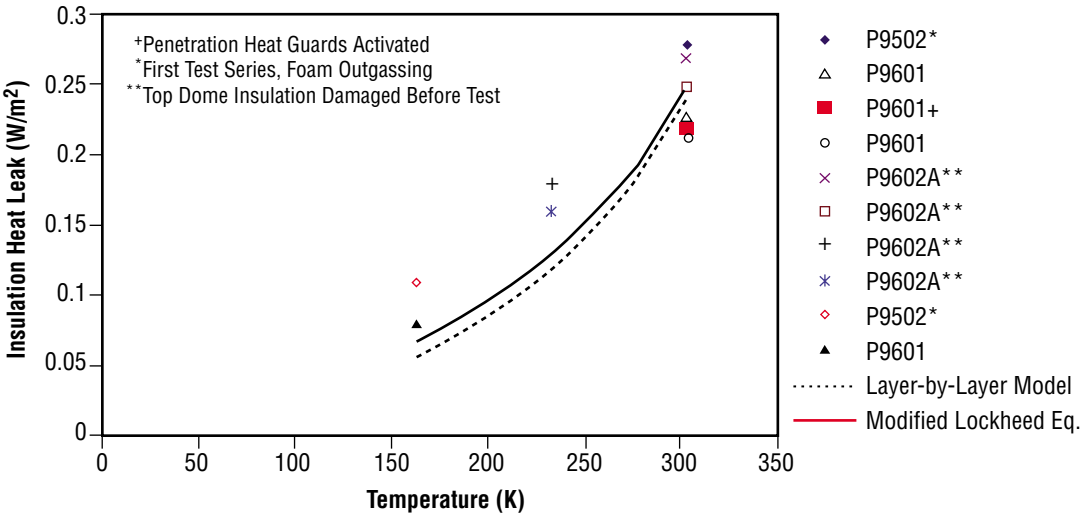

Figure 20. Heat leak modeling correlations with test data, 45 layers VD-MLI.

5.2 Application Examples

To illustrate the advantages and weight redution benefits of using VD-MLI for the storage of LH_2, two examples are considered and the results are presented in the following sections.

5.2.1 Performance Versus Number of MLI Layers

To assist in visualizing VD-MLI applications to other situations, performance variations with the number of MLI layers (30-, 60-, and 75-layer blankets) were modeled and results are presented in figures 21–23, respectively. The individual insulation components or layers have the same physical and thermal properties as those within the MHTB 45-layer foam/VD-MLI system. Also, in each case, the layer densities for each of the three MLI segments (refer to fig. 19) are identical to those with the MHTB; i.e., are 8, 12, and 16 layers/cm for segments one, two, and three, respectively. Unlike the MHTB insulation, an equal number of layers are assumed in each segment; however, it should be noted that the model is not constrained to this assumption and a varying number of layers in each segment can be used instead. The heat leak results with both the layer-by-layer and modified Lockheed model simulations are almost identical and consistently remain within 6 percent. The predicted heat leak with the warm boundary at 305 K is about 0.362, 0.142, and 0.140 W/m^2 with 30, 60, and 75 layers, respectively. Thus, the benefits of increased layers became insignificant above 60 layers.

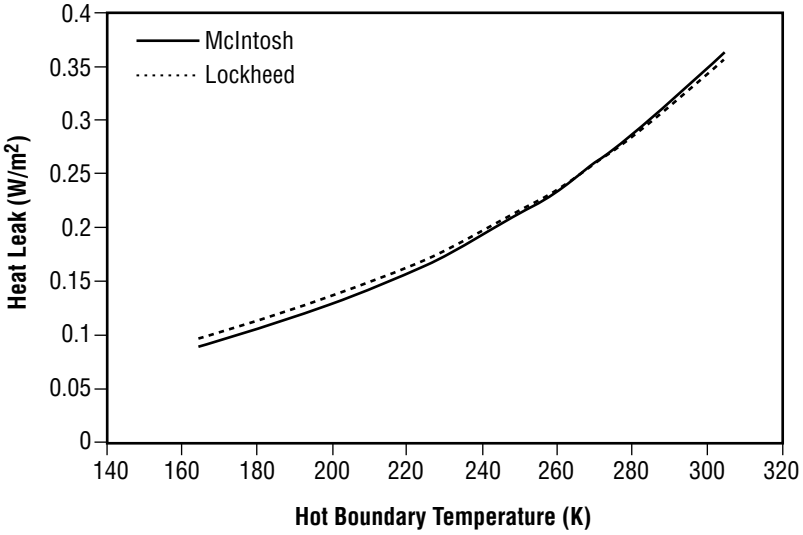

Figure 21. Heat leak predictions for 30 layers VD-MLI.

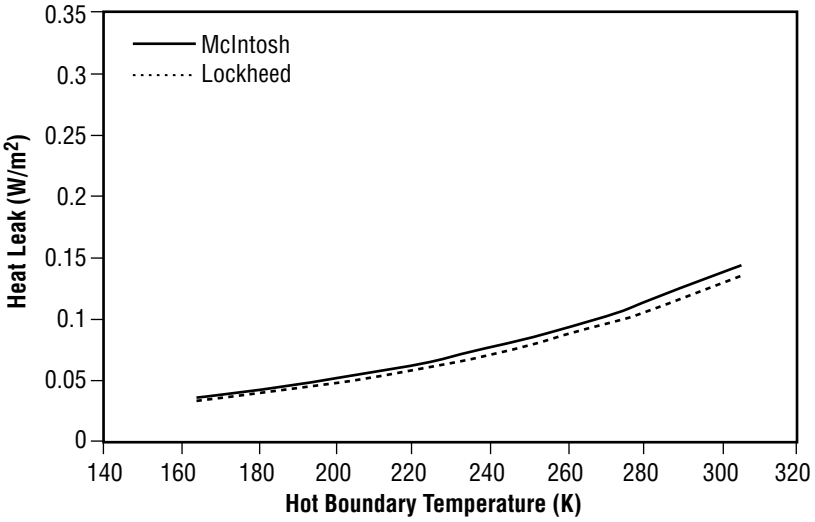

Figure 22. Heat leak predictions for 60 layers VD-MLI.

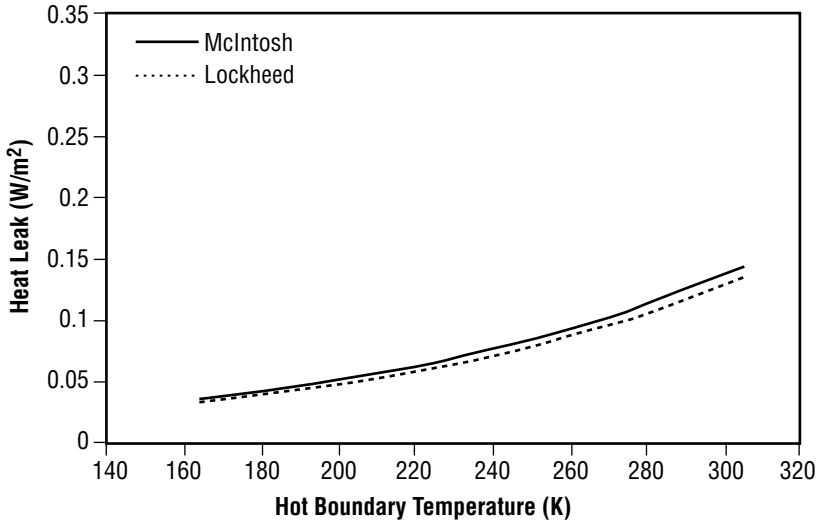

Figure 23. Heat leak predictions for 75 layers VD-MLI.

5.2.2 Example Upper Stage Application

Example data illustrating the benefits of applying VD-MLI to a Centaur G Prime upper-stage LH_2 tank with 0.25-mil DAM are presented in table 4 for a 45-day mission. With a tank surface area of 81.6 m^2, the weight difference between the 45-layer VD-MLI and "standard Lockheed model" MLI blanket would be 43 kg (VD-MLI weighs 41 percent less) if the boiloff is held constant. Conversely, if the blanket weights are held constant, the 45-day mission boiloff is 159 and 382 kg with the VD-MLI and standard MLI, respectively; i.e., the VD-MLI boiloff was 58 percent less than that with the standard blanket.

Table 4. Variable density and standard MLI application comparison.

Upper Stage LH_2 Tank MLI Application Examples, 305 K Boundary Temperature			
MLI System 1/4-mil Aluminum Mylar Layer	**Applied MLI Weight (kg)**	**45-Day Boiloff (kg)**	**45-Day Boiloff (%)**
Variable density MLI	57	159	4.6
Standard MLI	56	382	11.0
Standard MLI	100	159	4.6

6. CONCLUSIONS AND RECOMMENDATIONS

An 18-m^3 hydrogen test article, termed the MHTB, was successfully utilized to experimentally evaluate the performance of a foam/MLI thermal control concept in the MSFC vacuum facility at test stand 300. The Isofoam SS–1171 SOFI was designed to protect against ground hold/ascent flight environments and enable the use of a dry nitrogen purge as opposed to the more complex/heavy helium purge subsystem normally required. The 45-layer MLI, designed for an on-orbit storage period of 45 days, included several unique features: a variable density MLI layup, larger but fewer DAM perforations for ascent venting, and roll-wrap installation of the MLI with a commercially established process. The VD-MLI roll-wrap installation process resulted in a very robust, virtually seamless insulation with an estimated man-hour savings of 2,400 hr per LH_2 and oxygen tank set (3-m diameter). Further, the installation concept enables a more repeatable, consistent product as compared to individually constructed MLI blankets.

The MSFC vacuum facility and associated controls performed very well, producing over 2,000 hr of testing. During orbital simulations, the vacuum was successfully maintained at 10^{-6} torr or less and the ullage pressure control system maintained LH_2 tank pressure within the prescribed ±0.00689 kPa (±0.001 psi).

Ground-hold testing produced the expected average heat leak of 63 W/m^2 at a foam surface temperature of 170 K. It is concluded that SOFI-type insulation is a feasible means for eliminating the need for helium purge-bag subsystems. Additionally, the foam reduced the influence of heat flux on effective propellant density; i.e., a hydrogen density degradation of <3 percent occurred as compared to 13 percent with MLI only and a helium purge.

Three orbit-hold test series were conducted to evaluate the VD-MLI performance with warm boundary temperatures ranging from 305 K to 164 K, with and without penetration heat guards, and with an off-nominal (damaged) MLI configuration in the last series. The first series yielded an insulation heat leak (total heat leak minus penetration heat leak) of 0.28 W/m^2 (9.75 W) with the warm boundary at 305 K. The three tests in the second series (P9601) yielded an insulation heat leak of 0.22 W/m^2 in each of three tests with the 305 K boundary. The lower heat leak observed in the second series is attributed to reduced outgassing, probably from the foam insulation. The third test series—conducted with damaged insulation—yielded insulation heat leaks of 0.27 and 0.25 W/m^2 with a 305 K warm boundary. Therefore, the insulation heat leak of 0.22 W/m^2 most closely represents the true insulation performance at the 305 K boundary condition. This translates into a boiloff loss of 0.117 percent per day. When compared to the best previously measured performance of a traditional MLI system, a 41-percent heat leak reduction with 25 fewer layers at the 300 K boundary condition was achieved.

Two analytical models were investigated for predicting VD-MLI performance, a “layer-by-layer” modeling methodology and a “modified Lockheed equation” spreadsheet model. Comparative analyses indicated that the model results were within 3 to 4 percent of each other. With the 305 K warm boundary condition, the insulation heat leak values predicted with the layer-by-layer model and modified

Lockheed equation were within 5 and 8 percent of the measured data, respectively. With the 164 K warm boundary condition, the model predictions were 30–34 percent below the measured data, but the practical effect is not significant since the heat leak was <0.1 W/m^2.

Therefore, either of the two models can be utilized in various mission applications to predict the performance of the MHTB-type SOFI/VD-MLI combination or the VD-MLI alone. During the development of analytical modeling for the VD-MLI, it was observed that larger, more widely spaced ventilation holes provided a significant radiation blockage advantage as compared to the standard, closely spaced smaller holes. The variable density contributed to a weight reduction or performance increase due to reduced conduction with fewer layers to perform the same task. The lack of seams, butt joints, and structural support pins no doubt contributed to the measured MHTB VD-MLI performance improvement as well.

To demonstrate application of VD-MLI to other situations, performance variations with 30, 60, and 75 MLI layers were modeled and indicated that the benefits of increased layers became insignificant above 60 layers. Also, as an example of upper-stage application, a Centaur G Prime LH_2 tank was evaluated for a 45-day mission using both VD-MLI and standard MLI blankets. With the boiloff held constant, the VD-MLI weighed 41 percent less than the standard MLI. Conversely, with equal blanket weights, the VD-MLI boiloff was 58 percent less than that with the standard MLI.

REFERENCES

1. Tein, C.L.; and Cunnigton, G.R.: "Cryogenic Insulation Heat Transfer," *Advances in Heat Transfer*, Vol. 9, pp. 349–417, 1973.

2. Martin, J.; and Hastings, L.: "Large-Scale Liquid Hydrogen Testing of a Variable Density Multilayer Insulation With a Foam Substrate," *NASA/TM—2001–211089*, Marshall Space Flight Center, AL, June 2001.

3. Fredrickson, G.O.: "Investigation of High-Performance Insulation Application Problems," McDonnell Douglas Astronautics Company–West, Final Report, Contract NAS8–21400, MDC G4722, August 1973.

4. Hedayat, A.; Hastings, L.; and Brown, T.: "Analytical Modeling of Variable Density Multilayer Insulation for Cryogenic Storage," *Advances in Cryogenic Engineering*, American Institute of Physics, Melville, NY, Susan Breon et al. (eds.), Vol. 47B, pp. 1557–1564, 2002.

5. McIntosh, G.E.: "Layer by Layer MLI Calculation Using a Separated Mode Equation," *Advances in Cryogenic Engineering*, Plenum Press, New York, Vol. 39B, p. 1683, 1994.

6. Keller, C.W.; Cunnington, G.R.; and Glassford, A.P.: "Thermal Performance of Multi-Layer Insulations," Lockheed Missiles & Space Company, Final Report, Contract NAS3–14377, 1974.

7. "Thermal Insulation Systems," *NASA Report N67–38580*, Chapter 4, Marshall Space Flight Center, AL, August 1967.

REPORT DOCUMENTATION PAGE

Form Approved
OMB No. 0704-0188

1. AGENCY USE ONLY *(Leave Blank)*	2. REPORT DATE	3. REPORT TYPE AND DATES COVERED
	May 2004	Technical Memorandum

4. TITLE AND SUBTITLE

Analytical Modeling and Test Correlation of Variable Density Multilayer Insulation for Cryogenic Storage

5. FUNDING NUMBERS

6. AUTHORS

L.J. Hastings,* A. Hedayat, and T.M. Brown

7. PERFORMING ORGANIZATION NAMES(S) AND ADDRESS(ES)

George C. Marshall Space Flight Center
Marshall Space Flight Center, AL 35812

8. PERFORMING ORGANIZATION REPORT NUMBER

M–1109

9. SPONSORING/MONITORING AGENCY NAME(S) AND ADDRESS(ES)

National Aeronautics and Space Administration
Washington, DC 20546–0001

10. SPONSORING/MONITORING AGENCY REPO NUMBER

NASA/TM—2004–213175

11. SUPPLEMENTARY NOTES

Prepared by the Vehicle and Systems Development Department, Space Transportation Directorate
*Alpha Technology, Inc.

12a. DISTRIBUTION/AVAILABILITY STATEMENT

Unclassified-Unlimited
Subject Category 16
Available: NASA CASI (301) 621–0390

12b. DISTRIBUTION CODE

13. ABSTRACT *(Maximum 200 words)*

A unique foam/multilayer insulation (MLI) combination concept for orbital cryogenic storage was experimentally evaluated using a large-scale hydrogen tank. The foam substrate insulates for ground-hold periods and enables a gaseous nitrogen purge as opposed to helium. The MLI, designed for an on-orbit storage period for 45 days, includes several unique features including a variable layer density and larger but fewer perforations for venting during ascent to orbit. Test results with liquid hydrogen indicated that the MLI weight or tank heat leak is reduced by about half in comparison with standard MLI. The focus of this effort is on analytical modeling of the variable density MLI (VD-MLI) on-orbit performance. The foam/VD-MLI model is considered to have five segments. The first segment represents the optional foam layer. The second, third, and fourth segments represent three different MLI layer densities. The last segment is an environmental boundary or shroud that surrounds the last MLI layer. Two approaches are considered: a variable density MLI modeled layer by layer and a semiempirical model or "modified Lockheed equation." Results from the two models were very comparable and were within 5–8 percent of the measured data at the 300 K boundary condition.

14. SUBJECT TERMS

orbital cryogenic fluid management, cyrogenic storage, cryogenic multilayer insulation, cryogenic foam insulation

15. NUMBER OF PAGES

44

16. PRICE CODE

17. SECURITY CLASSIFICATION OF REPORT	18. SECURITY CLASSIFICATION OF THIS PAGE	19. SECURITY CLASSIFICATION OF ABSTRACT	20. LIMITATION OF ABSTRACT
Unclassified	Unclassified	Unclassified	Unlimited